JOURNAL OF MATERIALS SCIENCE 30 (1995) 4316–4322

Effect of reinforcement size on age hardening of PM 2009 Al–SiC 20 vol % particulate composites

A.P. SANNINO, H.J. RACK
Materials Science and Engineering Program, Department of Mechanical Engineering, Clemson University, Clemson, SC 29634, USA

The influence of SiC particulate size on the age-hardening response of 2009 aluminium has been monitored utilizing hardness, electrical conductivity and differential scanning calorimetry. Ageing involved either two or three stages depending on the reinforcement size. For 2009 Al reinforced with 29 μm SiC_p, initial ageing consisted of GPB (Guinier Preston Baqaryatsky) I zone formation. Decreasing the particulate size to 4 μm eliminated GPB I formation. This suppression of GPB I formation during ageing suggests that decreasing SiC size decreases the vacancy supersaturation following quenching by providing additional vacancy sinks at SiC/matrix interfaces. Subsequent ageing involved, at the larger reinforcement sizes, a transition with increasing time from GPB I zones to GPB II–dislocation complexes. At smaller (4 μm) reinforcement sizes, the formation of GPB II–dislocation complexes occurs directly. Finally, the last stages of age hardening in all SiC_p-reinforced composites examined consisted of heterogeneous nucleation of S′/S and GPB II → S′/S transformation.

1. Introduction

During the last four decades, numerous investigations of age hardening in 2xxx Al alloys, whose Cu:Mg ratio is in the range 1.5:1 to 4.1:1 [1], have shown that the precipitation sequence generally involves supersaturated α (fcc) → GPB I zones → GPB II → S′ → S [1–9]. GPB I zones, which are related to AlMgCu (T), form by vacancy-aided solute diffusion. As such, the rate of solute clustering is extremely sensitive to quenching conditions, notably solution treatment temperature T_s, cooling rate, dT/dt, and the temperature difference between the solution treatment and quench temperature, ΔT. Increasing solution-treatment temperature, cooling rate and ΔT all promote retention of a higher vacancy supersaturation and therefore increase the rate of GPB I formation [2–5]. With continued ageing, ordered zones, designated GPB II, develop. These remain coherent with the matrix growing in the [1 0 0] matrix direction to form cylinders. Silcock [2, 3] observed this structure, which is related to $Mg_2Al_5Cu_5$, on the isothermal ageing temperature at 240 and 260 °C, the stability of this phase increasing with increasing Cu:Mg ratio (7:1 versus 2.2:1). Further ageing results in a rearrangement within the GPB I/II zones and leads to formation of an orthorhombic transition phase, S′. Using atomic resolution electron microscopy, Radmilovic *et al.* [9] reported that S′ heterogeneously nucleates at either clusters of magnesium and copper atoms or at subgrain/grain boundaries, growth being observed to occur by ledge migration. Eventually, S′ grows until it loses coherency with the matrix and S replaces it.

Similarly, the mechanical performance of 2xxx alloys has been shown to be enhanced through the incorporation of hard ceramic particulates or whiskers [10, 11] ; moreover, influences of reinforcement on the microstructure and age-hardening response of the 2xxx alloys may be expected. Although investigations of 2xxx Al–SiC have reported that the presence of ceramic reinforcements in aluminium does not significantly modify the aluminium alloy ageing sequence, precipitation kinetics [12] and volume fractions of precipitation [12, 13] have been shown to be altered. This result is not restricted to 2xxx (Al–Cu–Mg) metal matrix composite (MMC) matrices [12–16] but also applies to other MMC matrices such as 6xxx (Al–Mg–Si), 7xxx (Al–Zn–Mg–Cu) [17–22] and 8xxx (Al–Li–Cu–Mg) [23], and is thought to be the consequence of the heavily dislocated DRA matrix, this substructure developing subsequent to solution heat treatment of SiC-reinforced aluminium alloys. The large, approximately 10/1, difference in the coefficient of thermal expansion (CTE) between the aluminium matrix and the SiC reinforcement causes differential straining at the reinforcement/matrix interface during quenching, with plastic relaxation leading to the generation of dislocations and numerous loops. It has been proposed [24] that the dislocation substructure may have two distinct, but interrelated, effects on DRA age hardening. These would be an increase in nucleation rate of a certain phase, e.g. S′/S in 2xxx matrix composites, to the detriment of others, e.g. GP zones, and an increase in precipitate growth rates through enhanced dislocation-assisted diffusion.

0022–2461

Further study, using differential scanning calorimetry to investigate the age-hardening precipitation reaction in SiC whisker (0–20 vol %) reinforced 2124 and 2219 aluminium composites [12], supports the proposal that the presence of a SiC reinforcement can lead to decreased formation of GPB zones; however, no distinction between GPB I and GPB II was reported. The reduction of GPB zone formation was thought by Papazian [12] to be due to a reduction in the retained supersaturated vacancy concentration in the composites *vis-à-vis* that of the unreinforced matrix. In addition, the same author suggested that a finer grain size and the incorporation of oxide particles due to the powder metallurgy (PM) process also contributed to the observed changes in precipitation kinetics.

Christman and Suresh [13], investigating the ageing response of a powder metallurgy 2124 Al–15 wt % SiC whisker composite also observed that the presence of the increased dislocation density facilitates the nucleation of S′, the intermediate strengthening precipitate. This, in turn, reduces the time for achieving peak hardness. Transmission electron microscopy revealed that, at any ageing time, S′ precipitate size was larger in the composite when compared with the unreinforced alloy. It was proposed that increasing dislocation density accelerates S and S′ precipitation, both known to nucleate heterogeneously, by increasing the number of available sites for nucleation, thereby increasing the apparent solute diffusivity in the matrix (e.g. [4, 5]).

Finally other studies in SiC-reinforced 2xxx aluminium showed that the matrix composition also has an influence on the effect of reinforcement on the ageing behaviour. For example, Rack [24] reported that reducing the magnesium content from 1.63 wt % to 1.34 wt % results in a 4 HRb decrease in peak hardness of the composites, the same effect being observed when the copper content is reduced from 4.6 wt % (2124 Al matrix) to 3.7 wt % (2048 Al matrix).

Although the effect of reinforcement presence [12–16] (most of the investigations dealing with whiskers), volume content [12], oxide presence due to the PM process [12, 15], and matrix composition [24] on the precipitation behaviour of discontinuously reinforced 2xxx aluminium alloys have been investigated, the influence of reinforcement particulate size on these phenomena has not yet been reported. However, reinforcement size has been shown to have a significant influence on the mechanical properties, ductility, toughness, fatigue life [11, 25–28], wear performance [29, 30], and deformation processing behaviour of SiC_p-reinforced composites [31]. The objective of the present work was therefore to identify the influence of particulate size, at constant volume fraction, on both the ageing sequence and the precipitation hardening behaviour of a 2000 series aluminium alloy reinforced with SiC particulates.

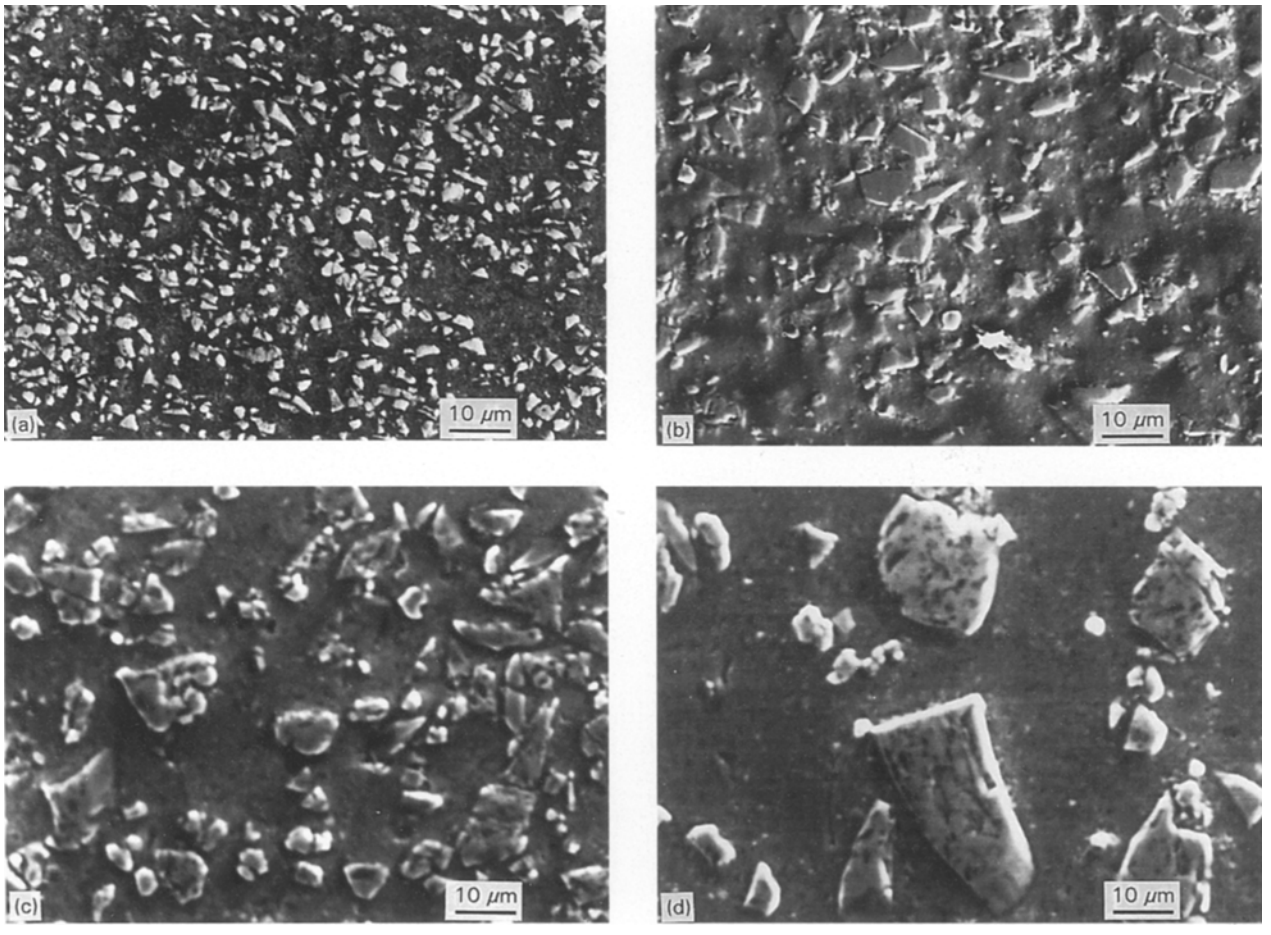

Figure 1 Scanning electron microscopy of the DRA samples: (a) 4 μm, (b) 10 μm, (c) 13 μm and (d) μm, the extrusion direction being normal to the micrograph surfaces.

TABLE I 2009 Al–SiC_p matrix chemical composition (wt %)

Nominal size (μm)	Cu	Mg	Fe	Si	SiC_p (vol %)
4	3.7	1.30	0.05	0.18	20.8
10	3.8	1.41	0.07	0.16	20.8
13	3.6	1.30	0.05	0.14	20.5
29	3.4	1.37	0.05	0.05	19.6

2. Experimental procedure

Four 2009 Al reinforced with 20 vol % SiC_p of varying reinforcement particulate size (Fig. 1), were fabricated by initial wet blending of pre-alloyed helium gas atomized powder. Following blending and drying, the composites were cold compacted to approximately 50% theoretical density and vacuum hot pressed in the mushy zone to 15.25 cm diameter billets. These billets were then homogenized for 96 h at 668 K and extruded to 12.7 cm wide by 1.27 cm thick plate bar, the extrusion ratio being 11.3:1. The 2009 alloy matrix composition together with the reinforcement volume fraction determined following extrusion is given in Table I.

The Particulate size measurements show that the variance, which characterizes the width of the size distribution, increases with increasing particulate size, Table II. Except for the smallest reinforcement size, an increase of variance is also observed for each composite after deformation, implying that the particulate-size distribution was broadened during fabrication. The latter observation, together with a decrease of average particulate size, implies that particulate fracture occurred during deformation. However, the extent of particulate-size reduction with deformation observed in this investigation is substantially less than that previously reported by Sun and Greenfield [32]. This difference in particulate fracture behaviour is believed to have resulted from a difference in extrusion die design. A stream-line flow die was employed for the 2009 composites examined in this study while standard shear-face dies were utilized by Sun and Greenfield, the former minimizing reinforcement damage when compared to a shear face die [10].

The investigation of the age-hardening response of the 2009 Al–SiC_p composites included macro-hardness, electrical conductivity and differential scanning calorimetry. Hardness/electrical conductivity samples, approximately 10 mm × 10 mm × 8 mm, were initially solution treated at 495 ± 2 °C for 1 h in a recirculating air furnace, followed by water quenching and immediate ageing. Artificial ageing was done at 150 ± 1 °C in an oil bath for ageing times between 0.5 and 1024 h.

Electrical conductivity measurements (% IACS, International Annealed Copper Standard), were performed prior to the hardness tests, with the hardness and electrical conductivity test surface lying perpendicular to the original extrusion direction, the test surface being polished to 600 grit and cleaned with acetone. Macrohardness data reported are the average of five measurements, the calibration of the Rockwell B apparatus being verified prior to each sample testing.

Finally, differential scanning calorimetry (DSC) analysis using a DuPont™ 2100 Thermal Analyser General V4.1C instrument were performed on DRA 3 × 3 × 0.5 mm plates immediately after solution heat treatment and water quenching. DSC results were obtained between 35 °C (after an equilibrium stage) and 400 °C, the DSC heating rate being 20 °C min^{-1}, with a pure aluminium disc of equal mass used as the reference (one of the pans serving as reference and the other containing the composite sample). Correction of the DSC thermogram to isolate the heat effect due to reactions occurring within the composite consisted of subtracting the heat flow ($W g^{-1}$), of the DSC reference, performed with high-purity aluminium in both pans, from the original DSC thermograms [7]. Assuming non-overlapping precipitation phenomena, the volume of the precipitate may be depicted by integrating the corrected DSC curves between the initial, T_i, and final, T_f, transformation temperature (i.e. $A(T_f)$ $KW g^{-1}$), divided by the heating rate, $\phi(K s^{-1})$, which gives the heat effect, H ($J g^{-1}$). The volume of precipitate is proportional to the heat effect per gram of sample, i.e. the thermal energy per gram of sample ($J g^{-1}$), taken from the surroundings to form a precipitate [33].

Kinetic analysis of low-temperature ageing was performed according to the method presented by Jena *et al.* [7] assuming that dY/dT can be expressed as

$$\frac{dY}{dT} = (1 - Y)\frac{k_0}{\phi}\exp\left(-\frac{Q}{RT}\right) \quad (1)$$

TABLE II Statistical description of SiC reinforcements in 2009 Al–SiC_p composites

	Before deformation[a]		After deformation[b]	
Nominal size (μm)	Mean diameter, $E(d)$ (μm)	Variance, $V(d)$ (μm^2)	Mean diameter, $E(d)$ (μm)	Variance, $V(d)$ (μm^2)
4	4.96	3.04	4.45	2.66
10	10.98	19.24	10.22	20.47
13	14.28	16.02	13.48	19.30
29	30.68	66.89	29.38	67.90

[a] Determined by sedigraphy assuming spherical particulates.
[b] Determined by quantitative microscopy.

where $Y(T)$ is the fraction of precipitate as a function of temperature, defined by

$$Y(T) = \frac{A(T)}{A(T_f)} \tag{2}$$

$A(T)$ representing the area under the peak between T_i and T ($T_i \leq T \leq T_f$), Q is the activation energy, k_0 is the frequency factor of the rate of formation dY/dt, and $\phi = dT/dt$, the heating rate [29].

3. Results

Ageing results of the SiC particulate-reinforced 2009 aluminium composites, as characterized by hardness and electrical conductivity measurements, are displayed in Figs 2 and 3, respectively. In the latter the electrical conductivity has been normalized as a function of time, t, to facilitate comparison between the various composites, C_t^n being defined as

$$C_t^n = \frac{C_t - C_0}{C_s - C_0} \tag{5}$$

where C_0 is the as-quenched conductivity, C_s is the conductivity at ageing time of 1024 h, and C_t is the conductivity at an ageing time t. Trends in Rockwell hardness and conductivity measurements are in good agreement, e.g. initial hardness increases were always accompanied by a drop in electrical conductivity.

Although the macrohardness of the four materials after quenching was similar, within a range of 67–69 R_b, the ageing kinetics were distinctly different. Materials containing smaller reinforcement particulate sizes, i.e. 4 and 10 μm, displayed a sluggish increase in hardness when compared to those reinforced with larger particulate sizes, i.e. 13 and 29 μm. Moreover, hardening appeared to proceed in three stages for the 13 and 29 μm particulate-reinforced 2009 composites, whereas two stages were observed for the smaller, 4 μm,

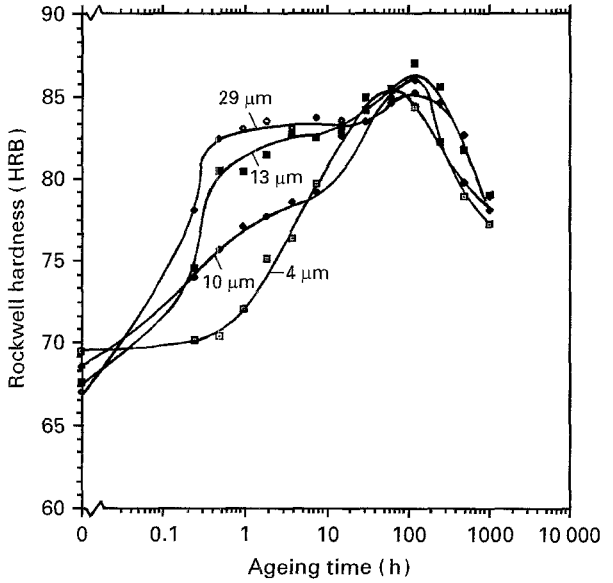

Figure 2 Age-hardening response of 2009 aluminium reinforced with 20 vol % SiC_p solution treated at 495 °C for 1 h, water quenched and aged at 150 °C.

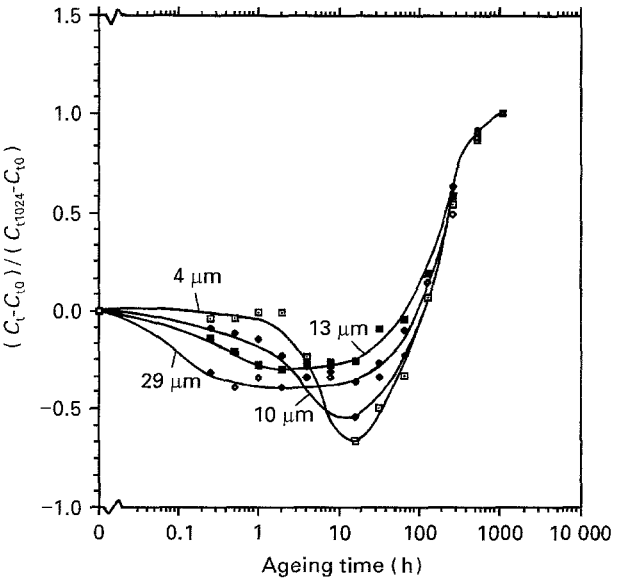

Figure 3 Normalized electrical conductivity of 2009 aluminium reinforced with 20 vol % SiC_p solution treated at 495 °C for 1 h, water quenched and aged at 150 °C.

reinforced composite. The initial stage for the larger particulate size composite involved an initial rapid hardness increase during early ageing times up to 0.5 h, followed by a slight hardness elevation and finally a further increase at longer times. It is also noteworthy that the larger the reinforcement particulate size, the higher the initial rate of age hardening, while the larger the reinforcement particulate size, the lower the rate of age hardening at intermediate ageing times. On the contrary, composites reinforced with 4 μm particulate showed little initial hardness change, followed by a substantial increase at ageing times beyond 1 h.

The time required for peak ageing was also a function of reinforcement size, approximately 64 h being required to achieve peak hardness in the 4 μm composite, while peak hardness in the other composites required ageing for 128 h at 150 °C. Ultimately, overageing was observed, the rate of hardness decrease being similar for all composites examined.

Accompanying electrical conductivity measurements, Fig. 3, mirror the hardness results. The 13 and 29 μm particulate-reinforced materials displayed an almost immediate electrical conductivity decrease upon ageing at 150 °C, this decrease corresponding to the major portion of the hardness increase (first stage). These reinforced materials then exhibited an essentially constant electrical conductivity until 16 h, coinciding with the moderate hardness increase (second stage during which only 3 R_b increase, from 82 R_b to 85 R_b within 63 h is detected), Fig. 3. Finally the conductivity again increased at longer times (third stage).

In contrast, changes in the electrical conductivity for the 4 μm reinforced composite was not detected until ageing time exceeded 1 h. Comparison of the changes in electrical conductivity and hardness measurements indicated that the decrease in electrical conductivity corresponded to the largest hardness increase (first stage). After 16 h ageing time, a continuous

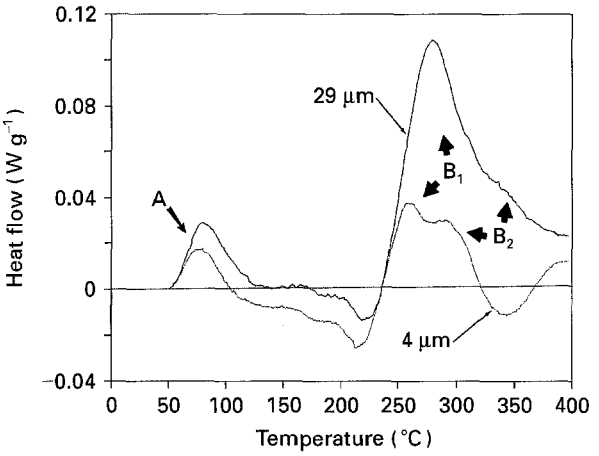

Figure 4 DSC thermograms of 2009 aluminium reinforced with 20 vol % SiC_p, particulate sizes of 4 and 29 μm, solution treated at 495 °C for 1 h, water quenched. DSC heating rate 20 °C min^{-1}.

TABLE III GPB formation kinetics analysis of 2009 aluminium reinforced with 20 vol % SiC_p solution treated at 495 °C for 1 h in an inert atmosphere and water quenched. DSC heating rate 20 °C min^{-1}

	2009–20% SiC_p 4 μm	2009–20% SiC_p 29 μm
Activation energy, Q (kJ mol^{-1})	115.2	90.3
Frequency factor, k_0 (s^{-1})	9.4×10^{17}	2.4×10^{14}
Heat effect, H (J g^{-1} sample)	2.14	3.32

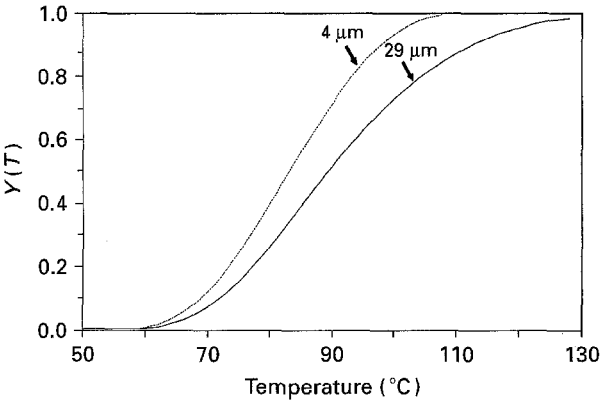

Figure 5 Fraction $Y(T)$ of GPB precipitate versus temperature of 2009 Al reinforced with 20 vol % 4 and 29 μm SiC_p.

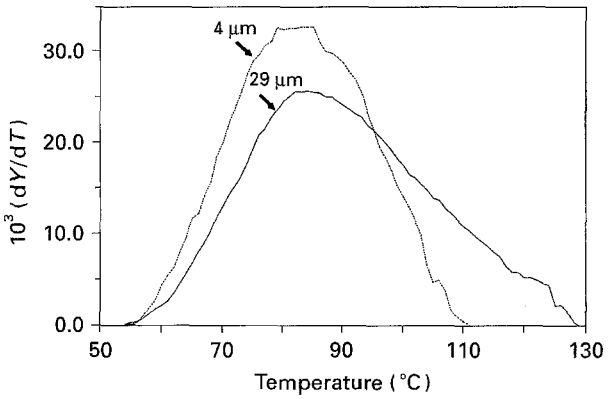

Figure 6 Rate of formation of GPB precipitation versus temperature of 2009 Al–4 and 29 μm SiC particulate composites.

electrical conductivity increase was observed while the rate of hardness increase diminished beyond 16 h (onset of second stage), Fig. 3.

Finally, the 10 μm particulate-reinforced material displayed a sharp electrical conductivity decrease between 8 and 16 h ageing time, similarly to the 4 μm particulate-reinforced composite, Fig. 3. This minimum was followed by an electrical conductivity increase which, as for the other composites, corresponded to peak and overageing.

Corrected DSC thermograms of 2009 Al reinforced with 20 vol % SiC_p are shown in Fig. 4, activation energies, Q, heat effect, H, and frequency factors, k_0, of GPB precipitation being reported in Table III. Several significant conclusions may be drawn from the DSC analysis. First, the volume fraction of the GPB zones, as represented by the area underneath curve A, or the heat effect, H, Table III, was significantly lower for the smaller 4 μm particulate-size composite when compared to the larger, 29 μm, reinforced composite. Second, ageing of the 4 μm composite displayed a clear separation of the S′ and S peaks, B1 and B2, while in the 29 μm particulate-size reinforced composite this separation was absent, Fig. 4. Moreover, the DSC thermogram showed that the volume fraction of combined S′/S precipitation in the composite reinforced with 29 μm SiC_p, as depicted by the area under curves B, was greater than that observed in 4 μm particulate-reinforced composite.

DSC kinetic analysis, Table III, indicated that the activation energy for GPB zone formation decreased with increasing reinforcement size. The total volume of the GPB zones per gram of sample, as depicted by the heat effect [7], Table III, also decreased with increasing reinforcement size. Fig. 5, representing the fraction of precipitate, $Y(T)$, for the 4 and 29 μm particulate composites as a function of ageing temperature, shows that GPB formation in the smaller particulate composite was completed at a lower temperature when compared to the larger particulate-reinforced material. In addition, the rate of precipitate formation, dY/dT, as a function of temperature, of both composites, Fig. 6, reached their maximum at the same temperature, approximately 85 °C. Below 95 °C, the rate of formation was higher for the 4 μm composites than for the 31 μm composite, the contrary being observed between 95 and 130 °C.

4. Discussion

The results of this investigation indicate that the precipitation sequence normally exhibited by 2xxx Al alloys, i.e. supersaturated α (fcc) → GPB I zones → GPB II → S′ → S, is affected by SiC particulate size at constant volume fraction.

Fig. 2 shows that the hardness increase may involve either two or three stages depending upon SiC particulate size. For example, the 29 μm SiC-reinforced

composite exhibited a higher initial rate of age hardening, while the smaller, 4 μm, particulate-reinforced composite did not exhibit any evidence for precipitation during the first hour of ageing. This behaviour was confirmed by electrical conductivity measurements, Fig. 3. The electrical conductivity of the 29 μm composite decreases at the shortest ageing times, while the electrical conductivity in the 4 μm composite was unaffected by ageing at times less than 2 h. This initial decrease in electrical conductivity has been shown by Rosen *et al.* [34] to be associated with GPB I zone formation. Therefore, the absence of an initial decrease suggests that the extent of GPB I zone formation is significantly decreased at the smallest SiC size. This decrease in GPB I zone content, as indicated by hardness and electrical conductivity measurements, is consistent with the DSC results, Fig. 4. Indeed, the volume fraction of the GPB zones was significantly lower for the small particulate size, 4 μm, material when compared to the larger, 29 μm, composite.

Kim *et al.* [35], investigating the precipitation behaviour of an Al–4 wt % Cu/ 5–15 wt % SiC_w composite, similarly observed suppression of the θ" (or GP II) formation, and suggested that this effect was related to the high dislocation density with the composite material. The suppression of GPB I zone formation during ageing in the 4 μm SiC-reinforced composite cannot, however, be associated with this increase in dislocation density. This proposal would require that the dislocation density be a function of particulate size; however, Dutta and Bourell, using continuum mechanics and finite element analysis, have shown that for 20 vol % DRA composites reinforced with SiC particulates larger than 1 μm, the plastic zones overlap [36, 37] and that, at a fixed reinforcement volume fraction, the amount of plastic strain, and therefore the matrix dislocation density, is not expected to be dependent on the reinforcement size.

Similarly, the decrease in vacancy supersaturation associated with GPB I zone suppression in 4 μm reinforced DRA cannot be due to powder oxide/matrix interface vacancy trapping, as suggested by Papazian [12] or Lee *et al.* [15], all composites having been processed in a similar fashion.

The decrease in vacancy supersaturation may, however, be related to the increase in SiC/matrix interfacial surface area with decreasing SiC_p size, these interfaces serving as vacancy sinks during quenching. As depicted schematically in Fig. 7, at equivalent volume per cent reinforcement, the total reinforcement/matrix surface area will increase with decreasing particulate size. Therefore, the larger interfacial area in the finer particulate-reinforced composite system should provide an increased number of vacancy sinks. The latter would decrease the vacancy supersaturation, thereby decreasing the extent of GPB nucleation, and, in turn, the level of precipitation hardening due to GPB I zone formation. Finally, the intermediate size (10 and 13 μm) reinforced composites, exhibited initial intermediate rates of hardness increase and rates of electrical conductivity decrease and appear to be transition cases between the two extremes, 4 and 29 μm reinforced materials.

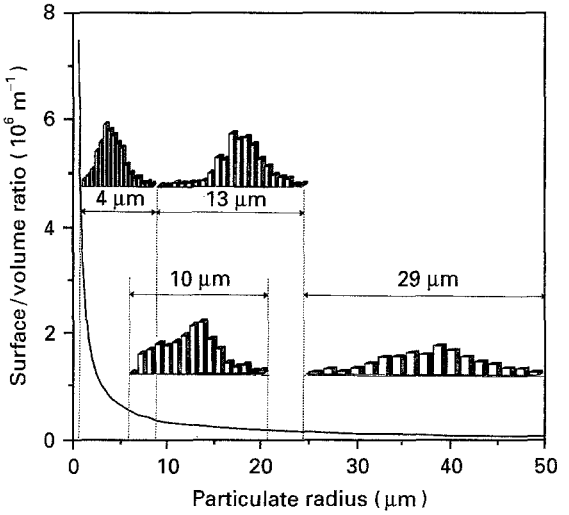

Figure 7 Surface/volume ratio as a function of particulate size and distribution.

Based on the previous considerations, it is proposed that strengthening of the 4 μm reinforced material during underageing is principally provided by GPB II–dislocation complex formation [7]. In contrast, the rapid age hardening and decrease in electrical conductivity during the first hour of ageing (first stage) suggests that GPB I zone strengthening is predominant in the 29 μm particulate composite. The second stage of age hardening is then, for the 29 μm composite, related to the transformation GPB I zones to GPB II. The latter transformation, involving only a structural modification in the zones, does not significantly affect either the hardness or the electrical conductivity. The 10 and 13 μm particulate-reinforced composites again appear to be intermediate cases having a peak hardness higher than the other composites, the hardness increasing and electrical conductivity decreasing continuously during initial ageing. This suggests that strengthening for these materials is provided by combined GPB I– and GPB II–dislocation complexes. More generally, particulate size decrease is associated with gradual substitution of GPB I zones by GPB II–dislocation complexes as the main strengthening agent.

Finally, the DSC results show that the 4 μm material displayed an enhanced separation of the S′ and S peaks when compared to the 29 μm particulate-size composite; however, due to the overlapping precipitations of S′ and S, no kinetics analysis allowing further explanation was possible. Also, the DSC thermogram shows that the volume fraction of combined S′/S precipitation in the composite reinforced with 29 μm SiC_p is greater than that observed in 4 μm particulate-reinforced composite. This suggests, in combination with Fig. 2, where the peak hardness values of both composite materials are essentially identical, that the S′/S strengthening precipitates in the large particulate-reinforced composite are coarser than in the 4 μm reinforced composite.

Summarizing, initial ageing in 2009 Al–SiC particulate composites consists of GPB I zone formation assisted by vacancy supersaturation from the aluminium

copper magnesium solid solution, the extent of the $Al_{ss} \rightarrow$ GPB I transformation decreasing as particulate size decreases. Longer ageing times involve, for larger reinforcement size composites, transition of GPB I zones to GPB II–dislocation complexes. For small reinforcement size composites, the first stage is absent and the formation of GPB II–dislocation complexes occurs directly. The third stage of age hardening consists in heterogeneous nucleation of S′/S and GPB II $\rightarrow$ S′/S transformation [9].

5. Conclusions

Hardness, electrical conductivity measurements and differential scanning calorimetric analysis showed that reinforcement size in a 2xxx Al silicon carbide particulate composite has an influence on both the precipitation hardening behaviour and the ageing sequence.

Decreasing particulate size decreases the hardening rate during underageing while peak and overageing are not affected.

The ageing sequence of 2009 Al involves either two or three stages depending upon SiC particulate size.

1. Initial ageing in 2009 DRA composites consists in GPB I zone formation from a supersaturated Al–Cu–Mg solid solution, Al_{ss}. During this stage, the rate of hardness increase decreases with decreasing particulate size, the extent of the $Al_{ss} \rightarrow$ GPB I transformation decreasing as particulate size decreases. The decrease of GPB I zone formation during ageing in the smaller (4 μm) particulate-reinforced composite suggests that SiC size influences the vacancy supersaturation in as-quenched 2009 Al–20 vol % SiC_p composites. This decrease in vacancy supersaturation is proposed to be related to the increase in SiC/matrix interfacial surface area with decreasing SiC_p size, these interfaces serving as vacancy sinks during quenching.

2. Subsequent ageing involves, at larger reinforcement sizes, transition of GPB I zones to GPB II–dislocation complexes. At smaller reinforcement sizes, the first stage of age hardening is absent and the formation of GPB II–dislocation complexes occurs directly.

3. Finally, the third stage of age hardening, common to all particulate sizes 2009–SiC_p composites, consists of heterogeneous nucleation of S′/S and GPB II $\rightarrow$ S′/S transformation.

Acknowledgements

Financial support for this effort was provided by the National Science Foundation Tribology and Surface Engineering Division under grant MSS-91148551 supervised and monitored by J. Larsen-Bässe. The authors also thank Mr A. Walker, Advanced Composite Materials Corporation Inc., for supply of materials. The assistance of Professor M. Drews and Mrs K. Ivey, Textile Department, Clemson University, with thermal analysis is also acknowledged.

References

1. L. F. MONDOLFO, "Aluminum Alloys: Structure and Properties" (Butterworth, London, 1976).
2. J. M. SILCOCK, *J. Inst. Metals*, **89** (1961) 203.
3. *Idem, Acta Metall.* **8** (1960) 589.
4. D. A. PORTER and K. E. EASTERLING, "Phase Transformations in Metals and Alloys" (Chapman and Hall, London, 1992) p. 98.
5. D. TURNBULL, H. S. ROSENBAUM and H.N. TREAFTIS, *Acta Metall.* **8** (1960) 277.
6. J. M. PAPAZIAN, *Metall. Trans.* **12A** (1981) 269.
7. A. K. JENA, A. K. GUPTA and M. J. C. CHATURVEDI, *Acta Metall.* **37** (1989) 885.
8. J. YAN, L. CHUNZHI and Y. MINGGAO, *J. Mater. Sci. Lett.* **9** (1990) 421.
9. V. RADMILOVIC, G. THOMAS, G. J. SHIFLET and E. A. STARKE, *Scripta Metall.* **23** (1989) 1141.
10. H. J. RACK, *Adv. Mater. Manuf. Proc.* **3** (1988) 327.
11. A. L. GEIGER and J. A. WALKER, *J. Min. Metall. Mater. Soc.* **43** (1991) 8.
12. J. M. PAPAZIAN, *Metall. Trans.* **19A** (1988) 2945.
13. T. CHRISTMAN and S. SURESH, *Acta Metall.* **36** (1988) 1691.
14. A. P. SANNINO and H. J. RACK, unpublished research, Clemson University, Clemson, SC (1992).
15. H.-L. LEE, W.-H. LU and S. L.-P. CHAN, *Scripta Metall.* **26** (1992) 1723.
16. P. L. RATNAPARKHI, Master's thesis, Clemson University, Clemson, SC (1989).
17. MARY VOGELSANG, R. J. ARSENAULT and R. M. FISHER, *Metall. Trans.* **17A** (1986) 379.
18. M. TAYA and T. MORY, *Acta Metall.* **35** (1987) 155.
19. R. J. ARSENAULT and R. M. FISHER, *Scripta Metall.* **17** (1983) 67.
20. H. J. RACK and P. RATNAPARKHI, in "International Encyclopedia of Composites", Vol. 4, edited by S.M. Lee (Academic Press, New York, 1988) p. 378.
21. S. I. HONG and G. T. GRAY, *Acta Metall.* **40** (1992) 3299.
22. C. H. DAVIES, N. RAGHUNATHAN and T. SHEPPARD, *ibid.* **42** (1994) 309.
23. E. HUNT, P. D. PITCHER and P. J. GREGSON, *Scripta Metall.* **24** (1990) 937.
24. H. J. RACK, in "P/M Aluminum Matrix Composites", edited by Y.W. Kim and W.M. Griffith (Warrendale, PA,Minerals, Metals and Materials Society, 1988) p. 649.
25. W. H. HUNT, J. R. BROCKENBROUGH and P. E MAGNUSEN, *Scripta Metall.* **25** (1991) 15.
26. D. J. LLOYD, *Acta Metall.* **39** (1991) 59.
27. D. J. LLOYD and P. L. MORRIS, in "Science and Engineering of Light Metals", edited by K. Hirano, H. Oikawa and K. Ikeda (Japan Institute of Light Metals, Tokyo, 1991) p. 465.
28. W. H. HUNT Jr, O. RICHMOND and R. D. YOUNG, "ICCM and ECCM", Vol. 2, edited by F.L. Matthews, N.C.R. Buskell, J.M. Hodgkinson and J. Morton (Elsevier Applied Science, London, 1987) p. 208.
29. A. P. SANNINO, Master's thesis, Clemson University, Clemson, SC (1993).
30. A. P. SANNINO and H. J. RACK, *Wear*, in press.
31. S. GUILLARD, MS Thesis Clemson University, Clemson, SC (1991).
32. J. SUN and I. G. GREENFIELD, in "Proceedings of the Sixth International Conference on Composite Materials", edited by F.L. Mattews, N.C. Buskell, J.M. Hodgkinson and J. Morton (Elsevier Applied Science, London, 1987) p. 2.287.
33. T. DANIELS, "Thermal Analysis" (BIP Chemicals, Worcestershire, UK, 1973).
34. M. ROSEN, E. HOROWITZ, L. SWARTZENDRUBER, S. FICK and R. MEHRABIAN, *Mater. Sci. Eng.* **53** (1982) 191.
35. T. S. KIM, T. H. KIM, K. H. OH and H. I. LEE, *J. Mater. Sci.* **27** (1992) 2599.
36. I. DUTTA, S. M. ALLEN and J. L. HAFLEY, *Metall. Trans.* **22A** (1991) 2553.
37. I. DUTTA, D.L. BOURELL and D. LATIMER, *J. Compos. Mater.* **22** (1988) 829.

Received 13 July 1994
and accepted 21 February 1995